Finite Element Analysis of Thermo-Mechanical and Failure Properties of Hybrid Fiber Composites

S. BANERJEE and B. V. SANKAR

ABSTRACT

Multiphase composite material also known as hybrids have major engineering applications where strength to weight ratio, low cost and ease of fabrication are required. A high modulus material might need a replacement owing to its brittle nature leading to sudden failure. For example considerable reduction in cost without loss of mechanical properties can be obtained using Kevlar-graphite/epoxy systems. Advances in computational micromechanics allow us to study hybrid multiphase systems using finite element simulations. The goal of this research is to evaluate the effective mechanical properties of hybrid composites containing graphite and glass fibers interspersed in an epoxy matrix. Elastic constants such as longitudinal tensile and shear modulus and major Poisson's ratios seem to follow the RoHM (Rule of Hybrid Mixtures) relation with reasonable accuracy. Transverse modulus and transverse shear modulus can be predicted using the Modified Halpin Tsai relations for multiphase composites. Strength properties, unlike the elastic constants show high variability with random locations of the fibers for a given volume fraction. It is also observed that the stress corresponding to failure initiation of the hybrids were lower than that of graphite/ and glass/epoxy composites. This is due to the stress concentration caused by a second fiber inclusion. Effective coefficients of thermal expansion and residual thermal stresses are calculated for hybrid composites and compared with binary composites. Progressive damage model that uses damage mechanics based softening response for the matrix is used to model damage progression behavior for the hybrid composites. The damage evolution energy is equal to the fracture toughness of the epoxy. The results are compared to that of graphite and glass epoxy bi-material composite systems.

Sayan Banerjee, Graduate Student (sbanerjee@ufl.edu)
B. V. Sankar, Ebaugh Professor (sankar@ufl.edu)
Department of Mechanical and Aerospace Engineering, PO Box 116250, University of Florida, Gainesville, FL 32611, USA

INTRODUCTION

Hybrid composites are materials that contain more than one type of fiber in a single matrix material. Although, several such fibers can be incorporated, it has been shown that combination of two fibers will be beneficial [1]. They have been developed as a logical sequel to conventional composites containing one fiber since hybrid composites have features that can be used to meet various design requirements in a more economical way than bi-material composites. This is because expensive fibers like graphite and boron can be partially replaced by less expensive fibers such as glass and Kevlar [2]. It is also shown that transverse shear stress in hybrid composite beam can be lower than a laminated beam made of glass/epoxy or carbon/epoxy [3]. Moreover, hybrid composites can be tailored intelligently to fabricate a functionally graded material which has unique advantages such as better impact properties, fatigue strength and reduced thermal residual shock due to temperature gradient [4]. Some of the specific advantages of hybrid composites over conventional composites include better strength and stiffness, better thermal distortion stability, reduced weight and/or cost, improved fatigue resistance, reduced notch sensitivity, improved fracture toughness and/or crack arresting properties, and improved impact resistance [1].

Experimental techniques can be employed to study hybrid composites, however they are limited because it consumes significant time and resources. A computational model on the other hand can offer important insights into the effect of various fiber combinations and its effect on the overall properties, saving valuable designer time.

The mechanical properties of hybrid short fiber composites can be evaluated using the rule of hybrid mixtures (RoHM) equation, which is widely used to predict the strength and modulus of hybrid composites [5]. It is shown that RoHM type of equations can accurately predict the longitudinal modulus and to some extent the longitudinal strength. However, for the transverse and shear properties, due to the spatial variation of microstresses inside the RVE (representative volume element), RoHM is not effective. Strength values depend to a large extent on the fiber/matrix interaction and interface quality. In tensile testing, any minor (microscopic) imperfection on the specimen may lead to stress build-up and failure could not be predicted directly by RoHM equations [6].

The computational model presented in this paper takes into account, random fiber location inside a representative volume element for every volume fraction ratio of fibers, in this case, carbon and glass. Randomization of the fiber location for a given volume fraction has significant effect on the transverse properties. A progressive damage model that loads the specimen beyond the first element failure is analyzed to understand transverse strength of the hybrid composites. A ductile damage model is assumed for the matrix, which degraded the matrix properties assuming a given fracture energy dissipation. A Modified Halpin-Tsai relation is proposed for the transverse modulus and shear modulus. Finite element based micromechanics is used to obtain the results, which show a good match with experimental results for effective modulus for hybrid composites with ternary systems (two fibers and a matrix) [7]. Effective coefficients of thermal expansion (CTE) for the hybrid composites are evaluated and results compared with two fiber composites. It is also observed that thermal residual stress due to mismatch between

the fiber and matrix CTEs play a significant role in determining the strength of the composites.

COMPUTATIONAL MODEL FOR HYBRID COMPOSITE

Most practical unidirectional composites are transversely isotropic in the 2-3 plane (1 is referred to as the fiber direction) owing to the statistical randomness in fiber packing [8]. A hexagonal arrangement of fibers is modeled since it can represent transverse isotropy better compared to a square arrangement. There are 50 fibers in the RVE which allows for randomization of fibers. Hybrid composites are obtained by varying the number of carbon and glass fibers. In the schematic of the RVE shown green and red represent glass and carbon fibers, respectively, while the matrix is shown in white. The rectangular RVE is assumed to repeat itself in the 2-3-plane. Also, it is assumed that the radii of the fibers are equal and only the number of carbon and glass fibers within the RVE was varied to change the volume fractions. This gives us much more flexibility in creating the finite element mesh.

Since, the actual composite extends through the page in the longitudinal direction, a plane strain analysis is sufficient for the calculation of elastic moduli. A combined fiber volume fraction of 60% (V_{fg}+ V_{fc}=0.6) is assumed for all the composites analyzed in this paper. The proportions of the reinforcements have been varied to obtain five different hybrid composites. The volume fractions of glass and carbon fibers were determined as per (1)

$$V_{fg} = \left(\frac{N_g}{N_T}\right) * \ 0.6 \tag{1}$$

where, N_g = Number of fibers of glass
N_T = Total number of fibers in the RVE

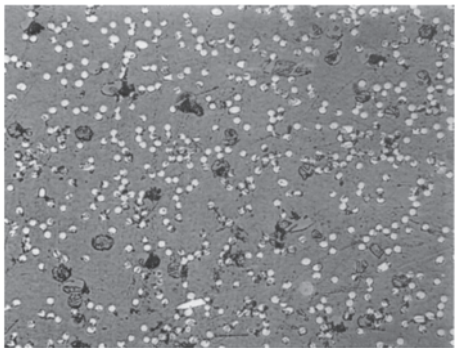

Fig 1. Cross section of a hybrid composite with V_f (carbon) = 18.75% and V_f (glass) = 6.25% [9]

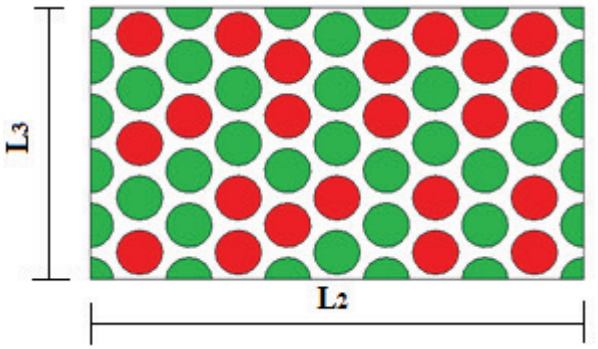

Fig 2. A representative volume element (RVE) for the hybrid composite

MICROMECHANICAL ANALYSIS

Elastic constants

The RVE of the hybrid composite was analyzed using the finite element method. Abaqus Standard CAE 6.9.2 was used for the analysis. It is assumed that a uniform macrostress exists through the composite. The subscript M in the subsequent equations refers to macrostress or macrostrain. The RVE is subjected to 6 macrostrains which are assumed to be uniform throughout the RVE. However, the microstresses which are the stresses in the constituent phases in the RVE will have spatial variation. The microstresses are volume averaged to calculate the macrostresses which are related to the applied macrostrains by the constitutive relation given by (2)

$$\{\sigma^M\} = [C]\,\{\varepsilon^M\} \tag{2}$$

where, $[C]$ is the stiffness matrix of the homogenized composite. For each applied non-zero macrostrain, it is also subjected to periodic boundary conditions such that all other macrostrains are zero. The six cases are [10]: Case 1: $\varepsilon_{11}^M = 1$; Case 2: $\varepsilon_{22}^M = 1$; Case 3: $\varepsilon_{33}^M = 1$; Case 4: $\gamma_{12}^M = 1$; Case 5: $\gamma_{13}^M = 1$; Case 6: $\gamma_{23}^M = 1$. Banerjee et al. has a table listing the periodic boundary conditions [journal paper]. The effective elastic constants of the composites can be obtained from the $[C]$ matrix.

Thermal analysis

For calculating the effective coefficients of thermal expansion, the RVE is subjected to a uniform temperature change ΔT with the boundaries on rollers such that the macrostrain is zero. The microstresses at the constituents can be volume averaged to calculate the macrostress, which is related to ΔT by (3)

$$\{\alpha\} = \frac{1}{\Delta T}[C]^{-1}\{\sigma^M\} \tag{3}$$

where, $\{\alpha\}$ is the matrix of effective thermal coefficients of the composites. Since all the composites including the hybrids are transversely isotropic in the 2-3 plane

α_2 was equal to α_3. The effects of hybridization and random fiber locations on the thermal coefficients were studied and the results are shown later.

The mismatch of the coefficients of thermal expansion between the different phases results in development of thermal stresses which are not accounted for since the composite materials are often modelled as homogenous orthotropic material. Since, the curing of the composite is done at higher temperatures while the structural application is often intended at cryogenic temperatures, the composite is subjected to significant thermal load. These stresses known as thermal residual stresses are evaluated for all the composites in this study. In order to calculate the thermal residual stress two steps are followed. Firstly, the composite is subjected to microstresses at the constituent level from the application of the thermal load, ΔT, for calculation of CTEs. The next step would be to apply a uniform macrostrain such that the RVE can expand freely. If the microstresses due to these two steps are added, the thermal residual stresses at the constituent level can be computed, although the volume average of the microstresses should be equal to zero. The effect of hybridization on thermal residual stress has been shown later.

Strength properties

The micromechanical failure analysis procedure also known as the Direct Micromechanics Method (DMM) can be used to predict the effective strengths of the composite [11]. This method checks every constituent element in the fiber and matrix level for critical stress for a given state of macrostress. The first occurrence of failure is treated as overall failure of the composite. Although conservative, this gives an estimate of the initiation of failure. In this study, a maximum principal stress failure criterion is used for glass and epoxy material while Hashin's failure criterion is used for the carbon fiber [12]. The interface is assumed to be perfect with no failure of the interface.

Progressive damage

The DMM gives us a conservative estimate of strength, which is informative but does not represent the ultimate failure of the composite. Typically epoxy matrix composites are ductile in nature and show elastic-perfectly plastic behavior before softening and failing completely. In order to simulate such a behavior, a ductile damage model built in Abaqus® is used for the epoxy matrix [13]. The epoxy initially follows a linear stress-strain behavior until it reaches the yield stress. Beyond that it is assumed that the epoxy is incapable of absorbing any more stress before the damage initiation point. The softening behavior of epoxy is governed by a linear damage law such that the energy dissipated in the softening regime is equal to the fracture toughness of epoxy. A general representation of damage model is shown in Figure 3. The fracture energy is calculated as shown in (4).

$$G_f = \int_{\bar{\varepsilon}_0^{pl}}^{\bar{\varepsilon}_f^{pl}} L\sigma_y d\bar{\varepsilon}^{pl} = \int_0^{\bar{u}_f^{pl}} \sigma_y d\bar{u}^{pl} \tag{4}$$

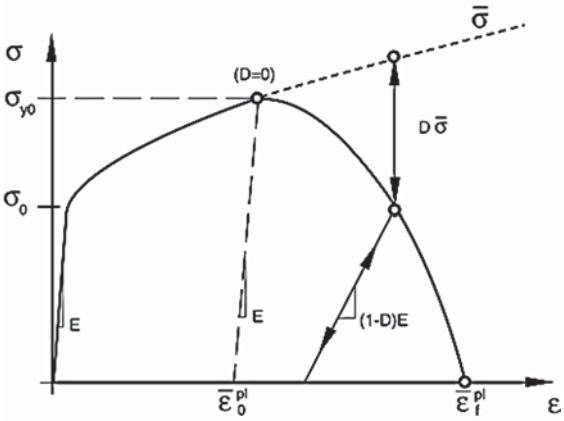

Fig 3. A general ductile damage model with strain hardening before softening [13]

L is the characteristic length of the element, which is length of a line across the element for a first order element. The results for transverse stress-strain behavior of the hybrids are compared with carbon-epoxy and glass-epoxy composites.

Finite Element Analysis

2D plane strain model with CPE3/CPE4 elements were used for evaluating the effective moduli and poisson's ratios, whereas shell elements with S3/S4 elements were used for the shear moduli. For the CTEs and damage models, 8 node solid elements were used. A unit cell and RVE model is shown in Figure 4.

RESULTS AND DISCUSSIONS

The material properties used for this study are shown in Table 1. Glass fiber and the epoxy matrix have isotropic properties whereas carbon fiber is transversely isotropic in the 2-3 plane. Hence, 5 independent elastic moduli are listed for all the materials. Strengths of the materials are listed in Table 2. Tensile and compressive strength for epoxy is 49 MPa and 121 MPa respectively, while shear strength is 93 MPa [11]. Although, the properties of the materials are chosen as close to the typical properties available, it should be noted that they are being used to solely study the effect of hybridization on different parameters. As such, this is more of a parametric study and the exact material properties used or generated are of less importance.

Table 1. Elastic moduli and strengths are in GPa units. CTEs are in ppm/C [11] [14]

Material	E_1	E_2=E_3	ν_{12}=ν_{13}	ν_{23}	G_{12}=G_{13}	α_1	$\alpha_2 = \alpha_3$
Glass	72.4	72.4	0.2	0.2	30.2	5	5
Carbon	263	19	0.2	0.35	27.6	-0.54	10.1
Epoxy	3.5	3.5	0.35	0.35	1.29	41.4	41.4

Table 2. Strengths of the constituents in MPa units [11]

Material	S_L^+	S_L^-	S_T^+	S_T^-	S_{LT}
Glass	1104	1104	1104	1104	460
Carbon	4120	2990	298	298	1760

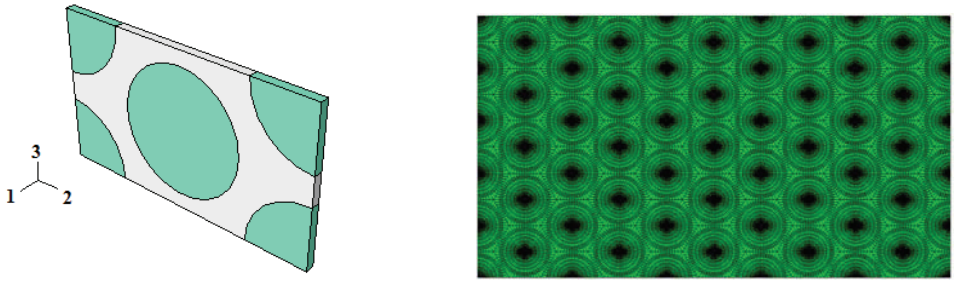

Fig 4. Schematic of unit cell and RVE

The elastic constants are plotted as a function of volume fraction of carbon varying from 0 to 0.6. It is observed in Figure 5 that the longitudinal modulus E_1 follows a linear relationship with volume fraction of carbon. The behavior can be predicted from the rule of hybrid mixtures (RoHM) type of equations given by (5).

$$E_1 = E_{1c}V_{fc} + E_{1g}V_{fg} + E_mV_m \tag{5}$$

where, V_{fc} and V_{fg} are volume fractions of carbon and glass respectively while V_m is volume fraction of matrix. Also, shown in Figure 5 is the variation of transverse modulus E_2 with V_{fc}. The transverse modulus and shear moduli have a non-linear behavior and can be accurately predicted by Modified Halpin-Tsai relation proposed by Banerjee and Sankar [15]. The relation is shown in (6). M_c and M_m are composite property and matrix property respectively, while η_i depends on M_{fi} which is the corresponding fiber property, i referring to carbon or glass. ξ is 1.16 for E_2 and 1.01 for G_{12}.

$$\frac{M_c}{M_m} = \frac{1 + \xi(\eta_c V_{fc} + \eta_g V_{fg})}{1 - (\eta_c V_{fc} + \eta_g V_{fg})}$$

where, (6)

$$\eta_i = \frac{\left(\frac{M_{fi}}{M_m}\right) - 1}{\left(\frac{M_{fi}}{M_m}\right) + \xi}$$

The variation of ν_{12}, ν_{23} and G_{23} can be found in [15]. The effective CTEs are also plotted as a function of V_{fc}. The plots are shown in Figure 6-8. In Figure 6(a), α_1 does not vary linearly with V_{fc}, but can be predicted from the relation (7) [8]. A direct implication of (7) is that, there exists a property $\alpha_1 E_1$, where E_1 is the

longitudinal modulus of the composite, which varies linearly with V_{fc} as shown in Figure 6(b).

$$\alpha_1 = \frac{\alpha_{1c}E_{fc}V_{fc} + \alpha_{1g}E_{fg}V_{fg} + \alpha_m E_m V_m}{E_{fc}V_{fc} + E_{fg}V_{fg} + E_m V_m} \tag{7}$$

$$\alpha_2 = (1+\nu_m)\alpha_m V_m + (\alpha_{1c}\nu_{12c} + \alpha_{2c})V_{fc} + (1+\nu_{fg})\alpha_{2g}V_{fg} - \alpha_1\nu_{12} \tag{8}$$

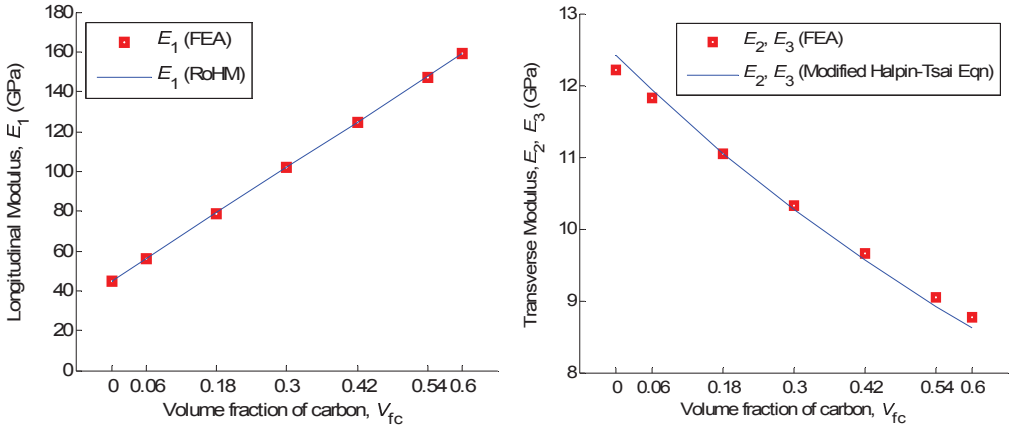

Fig 5. Longitudinal and transverse moduli for hybrid composites

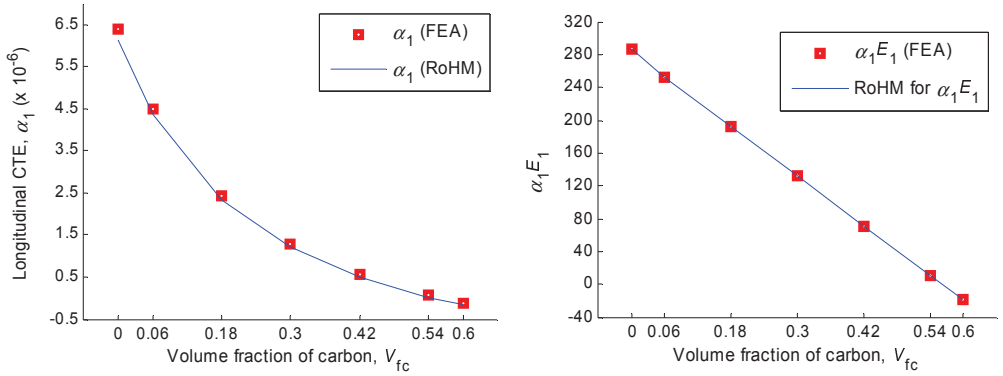

Fig 6 (a), (b). Longitudinal CTE and longitudinal thermal modulus for hybrid composites

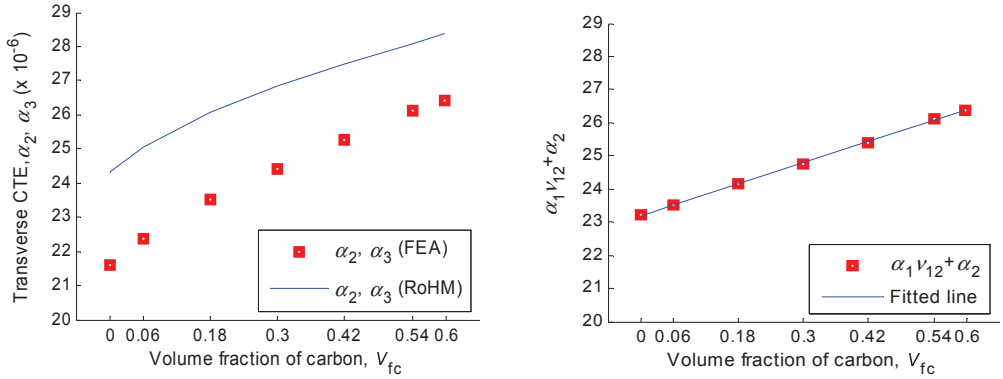

Fig 7 (a), (b). Longitudinal CTE and longitudinal thermal modulus for hybrid composites

Another property that is of interest is $(\alpha_1 \nu_{12} + \alpha_2)$. As seen in the Figure 7(b), it has a linear dependence on V_{fc}. Thermal residual stresses were studied for a unit change in temperature $(\Delta T = 1)$ for all the composites. It should be noted that the thermal residual stress, although a small fraction of the strength of the composite, could be significant for higher temperature differences. The maximum residual thermal stress occurs in the matrix due to mismatch of thermal expansion coefficient between the matrix and two fibers. In Figure 8 the maximum thermal residual von-mises stress and it's variability for random fiber location is plotted at the matrix as a function of V_{fc}. It can be observed that the maximum thermal residual stress and variability occurs for the composite with equal carbon and glass fibers. This is because for the composite with equal number of carbon and glass, there is a significant difference in thermal coefficients of the reinforcements and the matrix resulting in the high thermal residual stress. However, it was observed that although there was some variability in thermal residual stress due to random fiber locations, it was not very significant. The standard deviation and coefficient of variation is tabulated in Table 3.

Multi-axial failure envelopes were plotted based on the DMM approach for all the composites. The plots for hybrid composite were compared with carbon-epoxy (CFRP) and glass-epoxy (GFRP) composites. The hybrid composite considered for this study had equal proportion of carbon and glass fibers. The DMM method considers the first ply failure as the overall failure of the composite. Although conservative, this gives an idea of failure initiation in the composite. The bi-axial loading were applied in the $\sigma_1 - \sigma_2$, $\sigma_2 - \sigma_3$, $\sigma_2 - \tau_{12}$, $\sigma_2 - \tau_{13}$ and $\tau_{12} - \tau_{13}$ planes. For a given plane all other macrostresses were zero. The plots are shown in Fig 9 (a)-(e). The following observations can be made from the envelopes.

Table 3. Thermal residual stress in the matrix in MPa. μ and σ are mean and std. dev respectively

Hybrid	$\boldsymbol{\mu}$	$\boldsymbol{\sigma}$	$\boldsymbol{\sigma/\mu}$ **(%)**
H1	0.257	0.004	1.87
H2	0.264	0.004	1.89
H3	0.272	0.006	2.46
H4	0.267	0.005	1.81
H5	0.254	0.004	1.71

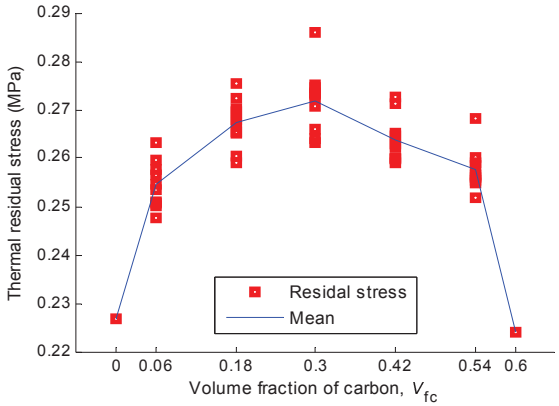

Fig 8. Thermal residual stress and variability for hybrid composites

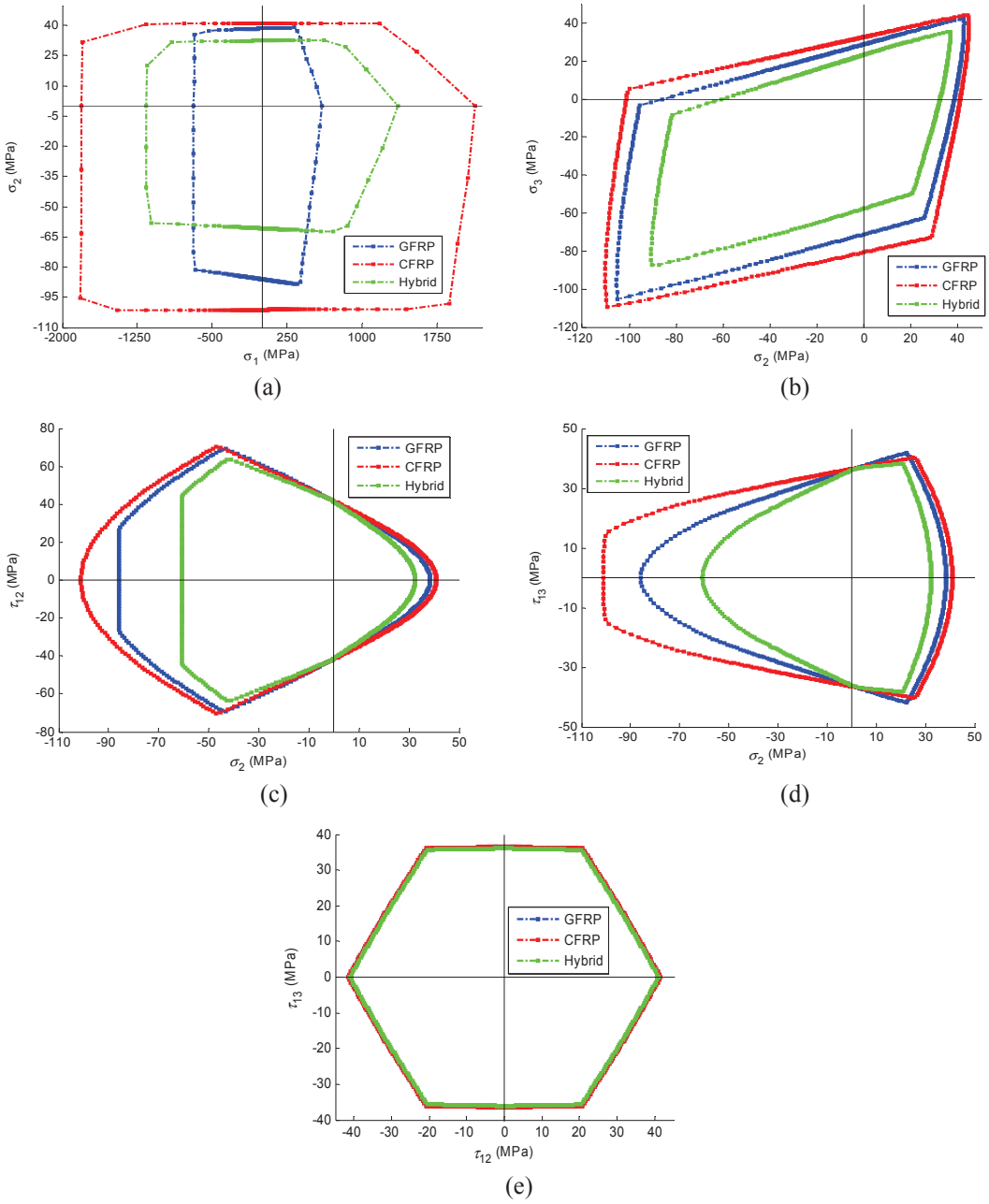

Fig 9. Bi-axial failure envelopes for hybrid composites

It can be seen in Figure 9(a) that the longitudinal strength of the hybrid is a weighted average of that of CFRP and GFRP. This is due to the fact that the longitudinal strength of the composite is proportional to E_1, which is also a weighted average of the longitudinal modulus of CFRP and GFRP. Moreover since epoxy has the lowest strain to failure among all the components, S_L^+ for the composites simply depend on the E_1 of the corresponding composite. For the transverse strengths, hybrids have lower strength than either CFRP or GFRP. The extra inclusion creates additional stress concentration in the matrix resulting in lower strength. Also, it was observed in Figure 9(b) that strength in the 3 direction is slightly lower than 2 direction although the moduli for the composites showed

transverse isotropy. This can be attributed to the unsymmetrical nature of the RVE in the 2 and 3 directions. From Figure 9(c)-(e), it can be observed that the longitudinal shear strengths, S_{12} and S_{13} are unaffected by hybridization and is dependent on the matrix tensile strength. As a result identical failure envelopes were observed in the $\tau_{12} - \tau_{13}$ plane for all the composites as seen in Figure 9(e).

Progressive damage is modeled for all the composites by considering a ductile damage model for the matrix as explained before. The RVE is subjected to boundary conditions such that a uniaxial macrostress is being applied in the 2 direction. The stress-strain response observed is shown in Figure 10. It can be observed that for the linear region of the stress-strain response is characterized by the corresponding transverse modulus of the composite. Once, the epoxy starts softening the fibers takes increasing load before the composite response becomes plastic. Also interesting is to note that irrespective of hybridization, all the composites soften nearly at the same stress. In order to understand the effect of hybridization 0.2% offset yield strength was calculated from the plots. Table 4 lists the strengths for hybrid composites. It can be observed that the strengths are significantly higher than those predicted using DMM. This is because of the load carrying capacity of the composite beyond the first ply failure. Also, it is observed that all the composites have very close transverse strengths which could be indicative of the fact that transverse strengths depend on the overall fiber volume fraction only.

Table 4. 0.2% offset yield strengths for composites

Composite type	**0.2% yield strength (MPa)**
CFRP	63.70
H1	63.75
H2	63.19
H3	63.35
H4	63.01
H5	63.20
GFRP	62.96

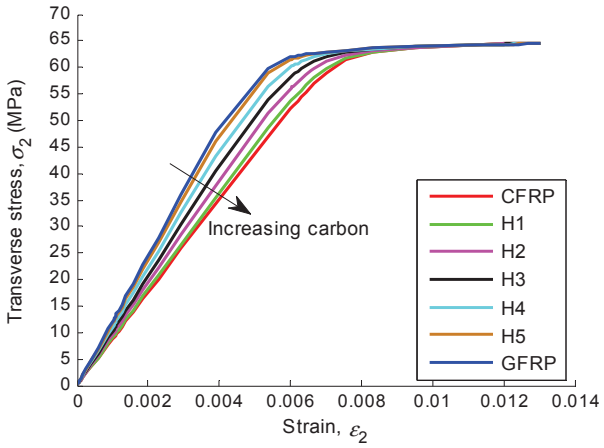

Fig 10. Transverse stress-strain response for the hybrid composites

CONCLUSION

A computational model for hybrid composites is being proposed with circular fibers in a hexagonal array. The overall fiber volume fraction is kept constant while varying the relative volume fraction of carbon and glass fibers. The fiber location has been randomized to study the variability in properties. Stiffness properties for the most part doesn't show any variability with fiber location for a given volume fraction. All the stiffness properties were calculated and compared with analytical predictive formulas.

Effective thermal coefficients of expansion were calculated for all composites and effect of hybridization was studied. The longitudinal thermal CTE can be predicted from RoHM type of equations and shows a good match with FEA results. However, the transverse CTE has been calculated but cannot be predicted accurately from existing analytical formulas. Thermal residual stresses were also calculated in the matrix phase and variability was studied for random fiber locations. It was shown that thermal residual stresses depend heavily on the mismatch of CTE between the reinforcements, and can be significantly high for large temperature differences. Since, composites are conventionally cured at elevated temperatures and find use at cryogenic temperatures, thermal residual stresses can play significant role in initiation of fiber microcracking and damage initiation.

Strengths of the composites were also studied. DMM method was applied to calculate the first ply failure strengths for the composites. It is observed that due to higher stress concentration owing to a second inclusion, hybrid composites have a lower transverse first ply strength. Also since the stress concentration is a point based phenomenon, transverse strengths show significant variability with location of fiber for a given volume fraction. A progressive damage model is proposed for the epoxy matrix which uses a ductile damage based damage mechanics model. The stress-strain behavior in the transverse direction is studied by the progressively loading the RVE beyond the first ply failure. It was observed that the 0.2% offset yield strength of the composites were nearly identical irrespective of the type and relative proportion of reinforcement used. However, a significant improvement in transverse strength for the composites was observed by using the progressive model as compared to the first ply failure strength which is typically a conservative estimate.

ACKNOWLEDGEMENTS

The authors sincerely acknowledge the partial support of United States Army Research Office grant W911NF-08-1-0120 and encouragement of Dr. C.F. Yen of ARL at APG, MD.

REFERENCES

1. Chamis, C. C., Lark, R. F.,"Hybrid composites – State-of-the-art review: Analysis, Design, Application and Fabrication", NASA Technical Memorandum, NASA, TM X-73545

2. Chou, Tsu-Wei, Kelly, Anthony, “Mechanical properties of composites.” Annu. Rev. Mater. Sci. 1980. 10:229-59
3. Song, M. C., et al. "Analysis of mode I delamination of< i> z</i>-pinned composites using a non-dimensional analytical model." Composites Part B: Engineering 43.4 (2012): 1776-1784
4. Sankar, B. V. "An elasticity solution for functionally graded beams." Composites Science and Technology 61.5 (2001): 689-696
5. Fu S.-Y., Xu G., Mai Y.-W., “On the elastic modulus of hybrid particle/short-fiber polymer composites”, Compos. Part B- Eng., 33, 291- 299, 2002
6. Mirbagheri, Jamal, Tajvidi, Mehdi, Ghasemi, Ismaeil, Hermanson, John C., “Prediction of the Elastic Modulus of Wood Flour/Kenaf Fibre/Polypropylene Hybrid Composites”, Iranian Polymer Journal, 16(4), 2007, 271-278
7. Chou, T. W. 1980 “Mechanical behavior of hybrid composites”, Emerging Technologies in Aerospace Structures, Structural Dynamics and Materials, ed. J. R. Vinson, New York: American Society of Mechanical Engineers
8. Gibson, Ronald. F., “Principles of Composite Material Mechanics”, Third Edition, CRC Press
9. Fu, Shao-Yun, Lauke Bernd, Mader, Hu Xiao, Yue Chee-Yoon, Mai Yiu-Wing, “Hybrid Effects on tensile properties of hybrid short-glass-fiber-and short-carbon-fiber- reinforced polypropylene composites”, Journal of Materials Science 36 (2001) 1243-1251
10. Zhu, H., Sankar, B. V., Marrey, R. V., “Evaluation of Failure Criteria for Fiber Composites using Finite Element Micromechanics”, Journal of Composite Materials, Vol 32, No. 8/1998
11. Stamblewski, Christopher, Sankar, B. V., Zenkert, Dan, “Analysis of Three-Dimensional Quadratic Failure Criteria for Thick Composites using the Direct Micromechanics Method”, Journal of Composite Materials, 2008; 42; 635
12. Hashin, Z., “Failure Criteria for Unidirectional Fiber Composites”, Journal of Applied Mechanics, June 1980, Vol. 47
13. Abaqus documentation® version 6.9.2
14. Choi, Sukjoo, Sankar, B. V., “Micromechanical Analysis of Composite Laminates at Cryogenic Temperatures”, Journal of Composite Materials, Vol. 00, No. 00/2005
15. Banerjee, S., & Sankar, B. V. (2014). “Mechanical properties of hybrid composites using finite element method based micromechanics”, Composites Part B: Engineering, 58, 318-327.